Angewandte Chemie

A Journal of the Gesellschaft Deutscher Chemiker

GDCh

International Edition

www.angewandte.org

Accepted Article

Authors: Luis M. Mateo, Qiang Sun, Shi-Xia Liu, Jesse J. Bergkamp, Kristjan Eimre, Carlo A. Pignedoli, Pascal Ruffieux, Silvio Decurtins, Giovanni Bottari, Roman Fasel, and Tomas Torres

This manuscript has been accepted after peer review and appears as an Accepted Article online prior to editing, proofing, and formal publication of the final Version of Record (VoR). This work is currently citable by using the Digital Object Identifier (DOI) given below. The VoR will be published online in Early View as soon as possible and may be different to this Accepted Article as a result of editing. Readers should obtain the VoR from the journal website shown below when it is published to ensure accuracy of information. The authors are responsible for the content of this Accepted Article.

WILEY-VCH

RESEARCH ARTICLE

On-surface Synthesis and Characterization of Triply-fused Porphyrin-graphene Nanoribbon Hybrids

Luis M. Mateo+, Qiang Sun+, Shi-Xia Liu, Jesse J. Bergkamp, Kristjan Eimre, Carlo A. Pignedoli, Pascal Ruffieux, Silvio Decurtins,* Giovanni Bottari,* Roman Fasel,* and Tomas Torres*

Abstract: On-surface synthesis offers a versatile approach to fabricate novel carbon-based nanostructures that cannot be obtained *via* conventional solution chemistry. Within the family of such nanomaterials, graphene nanoribbons (GNRs) hold a privileged position due to their high potential for a variety of applications. One of the key issues for their application in molecular electronics lies in the fine-tuning of their electronic properties through structural modifications, such as heteroatom doping or the incorporation of non-benzenoid rings. In this context, the covalent fusion of GNRs and porphyrins (Pors) represents a highly appealing strategy. In this work, we present the selective on-surface synthesis of a Por-GNR hybrid, which consists of two Pors connected by a short GNR segment. The atomically precise structure of the obtained dimer has been unambiguously characterized by bond-resolved scanning tunneling microscopy (STM) and noncontact atomic force microscopy (nc-AFM). The electronic properties of the dimer have been investigated by STS in combination with DFT calculations, which reveals a low electronic gap of 0.4 eV.

Introduction

During the last decade, on-surface synthesis has emerged as a powerful tool for the fabrication of novel nanomaterials.[1] Using this strategy, specific architectures are directly formed on solid surfaces via the covalent coupling of suitably designed precursors containing reactive units at specific positions of their molecular skeleton. The underlying surface, far beyond being a mere physical support, provides a two-dimensional (2D) confinement for the reactants, and selectively activates reaction pathways that are often not accessible by more "conventional" homogeneous or heterogeneous synthesis.[2] Additionally, and in contrast to the latter synthetic methods, on-surface synthesized nanostructures can be directly accessed by various surface-sensitive techniques such as scanning probe microscopy (SPM) allowing for a detailed "*in situ*" structural and electronic characterization of reactant, intermediate and product species with molecular or even chemical bond resolution.[3]

Since the seminal work by Grill and co-workers, demonstrating the successful on-surface covalent coupling of brominated porphyrins (Pors),[4] a number of nanostructures have been constructed using dehalogenative (Ullmann-type) coupling and other types of surface-assisted reactions.[5] Among the on-surface synthesized nanoarchitectures or molecules reported to date, low-dimension carbon-based conjugates constitute a particularly interesting class of materials. Thanks to their planar structure and highly π-delocalized electronic nature, they exhibit appealing properties for various technological applications.[6] Among others, graphene nanoribbons (GNRs) have gained a prominent position. Firstly reported in 2010,[7] atomically precise GNRs have been obtained by surface-assisted Ullmann-type polymerization and subsequent cyclodehydrogenation[8] of dibromo-substituted molecular precursors. Since then, GNRs with varying width,[9] GNR heterostructures,[10] and more recently, GNRs with zigzag edge topology[11] or with topological electronic quantum phases[12] have been fabricated through structural variations of the bromo-substituted precursors.

Remarkably, these GNRs present electronic properties that can be largely altered, by varying their topology, edge structure, and width.[13] A complementary approach to modify the electronic properties of GNRs is to "dope" them with heteroatoms such as nitrogen[14] or to include fused five-membered rings in their structure.[15] In this context, an interesting yet poorly explored strategy is fusing GNRs with molecular species that contain both five-membered rings and heteroatoms in their structures. Among the building blocks that fulfil these requirements, Pors stand out as ideal candidates due to their four pyrrolic units (*i.e.*, nitrogen-containing, five-membered rings), planar geometry and aromatic nature, rich redox chemistry, unique optoelectronic features and excellent long-range charge transport abilities.[16]

Interestingly, their electron transport ability, mainly explored in conjugated Por oligomers and polymers,[17] significantly depends on the type of inter-ring connection.[18] While connecting Pors through their *meso* positions with alkyne bridges results in moderate electronic communication between the macrocycles,[19] directly linking them through multiple covalent bonds, as in the case of triply-fused (*i.e.*, connected at their *meso-meso*, β-β, β-β positions) Por nanotapes,[20] produces stronger electronic conductivity. These latter conjugates have shown excellent electronic properties and a significant reduction in the highest occupied molecular orbital (HOMO)− lowest unoccupied

[a]   Luis M. Mateo, Prof. Tomas Torres, Dr. Giovanni Bottari
       Departamento de Química Orgánica, Universidad Autónoma de
       Madrid, Campus de Cantoblanco, 28049 Madrid, Spain
       and IMDEA-Nanociencia, Campus de Cantoblanco, 28049 Madrid,
       Spain and Institute for Advanced Research in Chemical Sciences
       (IAdChem), Universidad Autónoma de Madrid, 28049, Madrid,
       Spain.
       E-mail: giovanni.bottari@uam.es; tomas.torres@uam.es
[b]   Dr. Qiang Sun, Kristjan Eimre, Dr. Carlo A. Pignedoli, Dr. Pascal
       Ruffieux, Prof. Roman Fasel
       nanotech@surfaces Laboratory, Empa−Swiss Federal Laboratories
       for Materials Science and Technology, 8600 Dübendorf,
       Switzerland.
       E-mail: roman.fasel@empa.ch
[c]   Dr. Shi-Xia Liu, Prof. Silvio Decurtins, Prof. Roman Fasel
       Department of Chemistry and Biochemistry, University of Bern, 3012
       Bern, Switzerland.
       E-mail: silvio.decurtins@dcb.unibe.ch
[d]   Dr. Jesse J. Bergkamp
       Department of Chemistry and Biochemistry, California State
       University Bakersfield, 9001 Stockdale Highway, Bakersfield,
       California, USA
[+]   These authors contributed equally to this work.

       Supporting information for this article is given via a link at the end of
       the document.

WILEY-VCH

RESEARCH ARTICLE

molecular orbital (LUMO) gap upon increasing their length,[21] with some of the smallest gaps reported for organic compounds,[22] which makes them interesting molecular platforms to be used as molecular wires.

In this context, the realization and study of hybrid nanostructures constituted by "fused" Por and GNR fragments would be highly desirable and could, for instance, allow for the design of low-bandgap termini of GNRs for improved contacts in device integration. Additionally, the rich coordination chemistry of Pors[16b] would allow the realization of hybrid structures with controlled positioning of metal atoms along the GNR backbone. To the best of our knowledge, only few examples of "interfacing" GNRs with porphyrinoids have been reported to date.[23] One such hybrid[23a] consists of polymeric Por-GNR nanostructures obtained by on-surface Ullmann-type cross-coupling reaction between a dibromodianthracene derivative and a tetra(bromophenyl) FePor. However, the different reactivity and number of reactive units of the two co-deposited bromo-substituted precursors lead to a lack of control over important aspects in the Por-GNR polymer growth. In particular, the polydispersity, overall morphology, number of GNR "arms" fused around the Por core, or the symmetry of the resulting Por-GNR hybrid could not be controlled.

In the attempt to overcome some of these limitations, we report here the on-surface synthesis of a discrete and structurally-precise Por-GNR hybrid (**1**) formed via Ullmann-type coupling and subsequent cyclodehydrogenation of a suitably designed free-base Por precursor bearing a bromodianthryl moiety (**2**) (Scheme 1). The formation of triply-fused Por-GNR conjugate **1** was unambiguously demonstrated by high-resolution scanning tunneling microscopy (STM) and bond-resolved non-contact atomic force microscopy (nc-AFM) imaging. Hybrid **1** possesses a fully planar and π-conjugated structure resulting from the surface-catalyzed formation of 23 new C-C bonds (highlighted in red in Por-GNR **1**, Scheme 1). The electronic properties of **1** were characterized by scanning tunnelling spectroscopy (STS), showing the electronic orbitals originating from the GNR and the Por moieties. The experimental results are complemented by density functional theory (DFT) calculations performed with the CP2K code[24] within the AiiDA platform[25] (see Supporting Information for computational details).

Results and Discussion

Synthesis and X-ray Diffraction Studies of Por 2. The synthetic route to Por precursor **2** is described in Scheme 1. 9,10-anthraquinone (**3**) was reduced and dimerized with Zn under strongly acidic conditions to give dianthracene **4**, which was then brominated with *N*-bromosuccinimide (NBS) to give compound **5**.[26] Lithiation of the latter compound with *n*-BuLi and subsequent nucleophilic quenching with *N,N*-dimethylformamide gave the formylated dianthryl derivative **6** in a moderate yield, which was further brominated with NBS to obtain the aldehyde precursor **7**. Aldehyde **7** was then reacted with 2,6-dimethylbenzaldehyde in a statistical mixed aldehyde condensation reaction under classical Lindsey conditions[27] to give the target Por precursor **2** in 6% yield after chromatographic purification. The low yield is justified by the low reactivity of **7** in comparison with 2,6-dimethyl-benzaldehyde, which further lead to the formation of a considerable amount of tetra(dimethylphenyl)Por as side-product.

Scheme 1. Synthetic route to triply-fused Por-GNR hybrid **1**.[a]
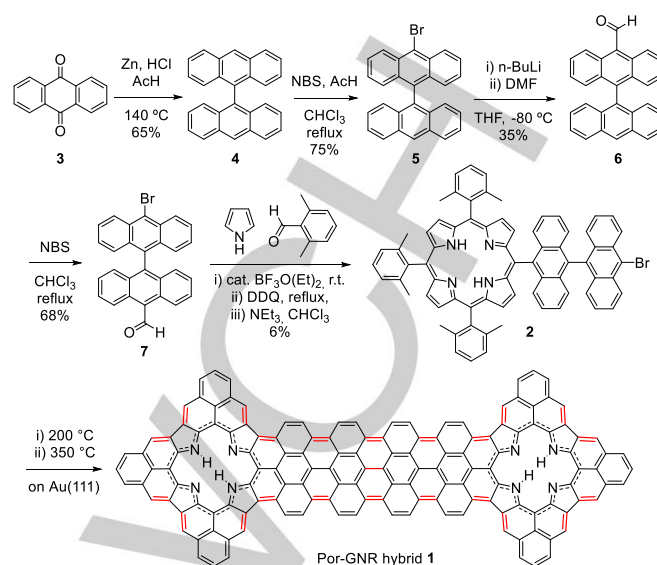
[a] For the sake of clarity, only one of the possible resonance structures of Por-GNR **1** is shown. Additional resonance structures can be found in Figure S1.31.

Por monomer **2** and all its precursors were characterized by ¹H and ¹³C NMR, high-resolution mass spectrometry, and UV-Vis spectroscopy (see Section 1 in the Supporting Information). Moreover, in the case of **2**, single crystals suitable for X-ray diffraction analysis were obtained by slow evaporation of a chloroform solution of this Por (Figure 1).
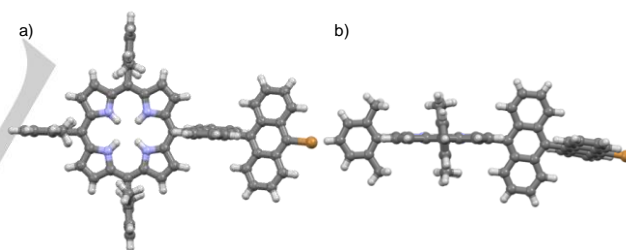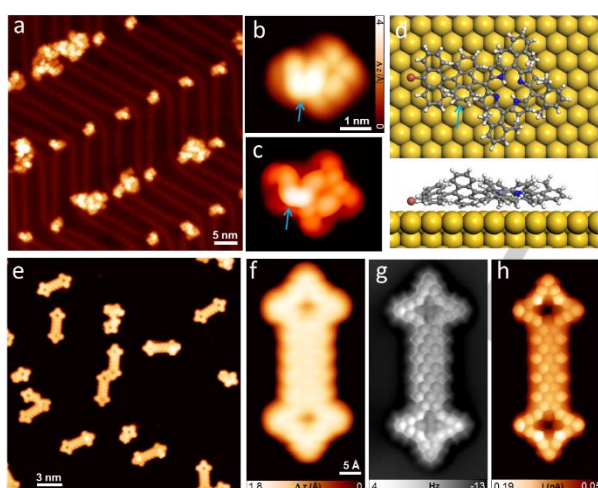

Figure 1. (a) Top and (b) side view (with respect to the Por macrocycle) of the X-ray crystal structure of Por **2**. Carbon atoms are in light grey, nitrogen atoms in light blue, bromine atom in orange, and hydrogen atoms in white. Chloroform molecules of crystallization have been omitted for clarity. Pyrrolic N-H hydrogen atoms are shown with 50% occupancy due to tautomerism.

An interesting feature of the crystal structure of **2** is the almost orthogonal arrangement adopted by the vicinal Por/anthryl and anthryl/anthryl subunits (*i.e.*, 89° and 78°, respectively). A similar arrangement is observed between the central Por core and the three peripheral 2,6-dimethylphenyl moieties. The highly non-planar structure of **2** is beneficial both for wet and on-surface chemistry. Firstly, it hampers the π-π stacking and increases the solubility, thus facilitating its purification and unambiguous characterization. Secondly, and more importantly, it provides a staggered geometry once deposited on Au(111), facilitating the on-surface Ullmann-type coupling reaction (*vide infra*).[28]

A Por analogous of **2** bearing one instead of two anthryl moieties (**8**) has been also synthesized as reference and its surface-assisted coupling leading to the formation of Por-GNR hybrid **9**

RESEARCH ARTICLE

investigated (see Supporting Information for its structural and on-surface characterization).
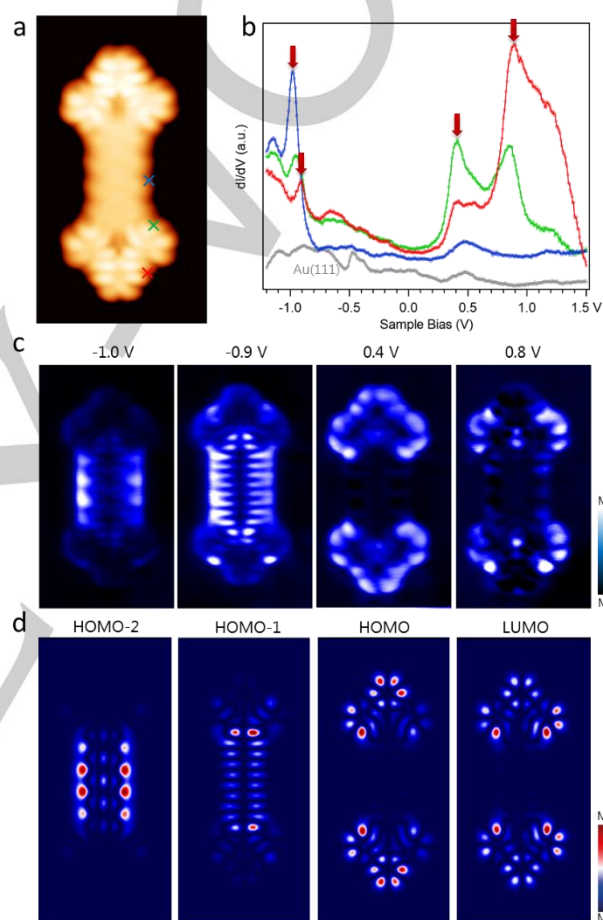
On-surface Reaction and Electronic Characterization. Prior to the on-surface reaction, the absorption of Por **2** on the Au(111) surface at room temperature was studied. As shown in Figure 2a, the molecules preferentially decorate the elbow sites of Au(111) and start to aggregate with increasing coverage. The close-up STM image of an individual Por **2** reveals a non-planar configuration of the molecule with an apparent height of ~4 Å (Figure 2b). This finding is also supported by DFT calculation of Por **2** on Au(111) which shows a distorted geometry between the vicinal Por/anthryl and anthryl/anthryl subunits (Figure 2d). Notably, the middle anthryl subunit, marked by an arrow in Figure 2d, has one peripheral benzene ring lifted farthest from the surface as a result of the steric hindrance between the neighboring anthryl and Por subunits. The corresponding STM simulation of Por **2** (Figure 2c) allows for a direct comparison with the experimental STM image (Figure 2b), which shows a very good match. Especially, the middle anthryl unit shows the highest contrast in excellent agreement with the experimental results. The dihedral angle between the two anthryl subunits of Por **2** on Au(111) is promising for the subsequent on-surface Ullmann-type dimerization.

apparent height of 1.8 Å, in good agreement with other graphene-based structures on surfaces (Figure 2f).[6b, 7-8] Bond-resolved non-contact atomic force microscopy (nc-AFM) successfully confirms the chemical structure of Por-GNR hybrid **1** (Figure 2g). Moreover, the simultaneously acquired constant-height current measurement ('CO STM imaging') displays a similar bond-resolved high-resolution image of the dimeric structure (Figure 2h). It is notable that some of the Pors are self-metalated with gold adatoms on the surface, which is reflected by an increased apparent height in the cavity of the Pors.[30] In the following, however, we focus on non-metalated Pors.


Figure 2. On-surface synthesis of Por-GNR hybrid **1**. (a) STM image after deposition of Por **2** on Au(111) held at room temperature (V_s = –2.1 V, I_t = 0.02 nA). (b) High-resolution STM image of Por **2** (V_s = –0.1 V, I_t = 0.3 nA) and (c) the corresponding STM simulation. (d) Top and side views of the DFT optimized geometry of Por **2** on Au(111). The blue arrows in (b), (c) and (d) indicate one peripheral benzene ring lifted farthest from the surface. (e) STM image of the sample after annealing to 350 ºC. (f) The close-up STM image of Por-GNR hybrid **1** (V_s = –0.5 V, I_t = 0.02 nA). The corresponding (g) bond-resolved nc-AFM image and (h) the simultaneously acquired current image (V_s = –5 mV, oscillation amplitude: ~80 pm).

Figure 3. Electronic properties of Por-GNR hybrid **1**. (a) STM image of Por-GNR **1** (V_s = 0.4 V, I_t = 0.5 nA) and (b) differential conductance dI/dV spectra taken at the positions indicated by crosses with corresponding colors in (a). Four prominent peaks around the Fermi level are highlighted by arrows. (c) Constant-current differential conductance maps recorded at the energies of the four prominent peaks. (d) Corresponding DFT-calculated LDOS maps of Por-GNR hybrid **1**.

The on-surface reaction was triggered by a two-step annealing process at 200 and 350 ºC, leading to the Ullmann-type C-C coupling and cyclodehydrogenation, respectively.[6b, 7-8] The cyclodehydrogenation temperature was kept below 360 ºC to avoid intermolecular dehydrogenative C-C coupling at high temperatures.[29] As shown in Figure 2e, the target Por-GNR hybrid **1** was successfully formed on the surface with a yield of ~30%. The close-up STM image of the hybrid **1** shows an

The electronic structure of Por-GNR hybrid **1** was studied by means of differential conductance (dI/dV) spectroscopy, giving access to its local density of states (LDOS). As shown in Figures 3a and 3b, point spectra taken at different positions of Por-GNR hybrid **1** reveal the presence of several peaks around the Fermi level. These correspond to the frontier molecular states of **1**, which are marked by arrows in Figure 3b. Spatially resolved dI/dV mapping, acquired at the corresponding bias voltages, was used

RESEARCH ARTICLE

to further identify these molecular states (Figure 3c). From the dI/dV mapping, it can clearly be seen that the two occupied states (–0.9 and –1.0 V) mainly originate from the quateranthene segment within Por-GNR hybrid **1**, while two unoccupied states (0.4 V and 0.8 V) result from the Por units. LDOS maps of the molecular states of **1** were simulated using DFT calculations in gas phase. The excellent matching of their overall shape with the experimental counterparts (Figures 3d and S2.1) suggests weak hybridization of molecular states with the substrate and thus allows comparing the energy levels of the calculated LDOS maps with the experimental ones. It is found that the map measured at 0.4 V is indeed related to HOMO of Por-GNR hybrid **1** and the one at –0.9 eV originates from the HOMO-1. This indicates a relatively large energy level re-alignment upon adsorption of dimer 1 on the Au(111) surface, with the gas phase HOMO becoming fully unoccupied due to charge transfer to the metal substrate.[31] Assuming negligible energy level renormalization, we can thus extract a (substrate screened) HOMO-LUMO transport gap of 0.4 eV of dimer **1** on Au(111), which is much lower than the 2.4 eV[32] of the surface-supported armchair GNR (AGNR) with a width of 7 carbon atoms (7AGNR). As a reference, the (optical) gaps of anthryl-fused Pors in solution are ~ 1.2, 0.77 and 0.61 eV for one,[33] two,[34] and four[35] anthryl units, respectively.

In addition to Por-GNR hybrid **1**, some non-coupled yet cyclodehydrogenated molecules were observed after the on-surface reactions (Figures 2e and 4). From the bond-resolved nc-AFM image, the dehalogenated, singly hydrogenated, and fully cyclodehydrogenated analogue of Por **2** can clearly be resolved (Figure 4b). This structure bears a special interest due to the existence of a zigzag end at the short 7AGNR segment, which is predicted to host a spin-polarized end state.[36] This end state of the 7AGNR on Au(111) features a finger-shaped LDOS pattern close to the Fermi level due to the fact that it is charged by the substrate.[36-37] In the constant-height CO-STM image acquired at a very small bias voltage (Figure 4c), the characteristic 7AGNR end state at the terminus of the planarized Por **2** is also observed, implying that the end state of 7AGNR does not hybridize with the Por unit.
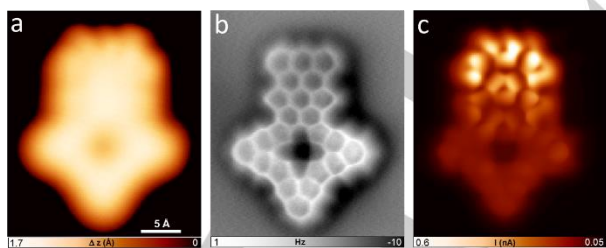
Figure 4. Structural characterization of dehalogenated, singly hydrogenated, and fully cyclized Por **2**. (a) STM image (V_s = –0.2 V, I_t = 0.05 nA) of the fully planarized Por **2**. The corresponding (b) nc-AFM image and (c) its simultaneously acquired current image (V_s = –5 mV, oscillation amplitude: ~80 pm).

To test the generality of the proposed synthetic route towards the preparation of Por-GNR hybrids, an analogous compound (*i.e.*, **8**) of Por **2**, bearing one instead of two anthryl moieties, has been also synthesized. The surface-assisted coupling of **8** indeed leads to the formation of a Por-GNR hybrid (*i.e.*, **9**) with a shorter

7AGNR segment (bisanthene) than Por-GNR hybrid **1** (see Supporting Information for more details). However, the overall reaction yield of Por-GNR dimer **9** is limited (less than 2%), which is tentatively attributed to steric hindrance (see Figure S2.5).

Conclusion

Herein, we report the surface-assisted synthesis of a novel Por-GNR hybrid (**1**) prepared by Ullmann-type coupling and subsequent cyclodehydrogenation reaction of an anthryl-substituted Por precursor (**2**) on Au(111), which was identified by high-resolution STM and nc-AFM imaging. The electronic structure of Por-GNR hybrid **1** was studied by dI/dV spectroscopy, proving the hybrid's fully π-conjugated nature. Using DFT calculations, the LDOS maps were simulated confirming the interpretation of the experimental data. Through these LDOS simulations, the electronic states have successfully been assigned, revealing a HOMO-LUMO gap of 0.42 eV for the hybrid **1**, which is much lower than solid-supported pristine 7AGNRs and significantly lower than anthryl-fused Pors in solution.

The presented work opens new pathways towards the preparation of further Por-GNR hybrid architectures. Some pathways of interest would be (i) the elongation of the GNR "spacer" to achieve Por "capped" GNRs with different lengths, and (ii) utilizing the metal complexation capabilities of Por macrocycles to produce Por-GNR hybrid materials doped with transition metals such as Zn, Cu, Co or Fe. Such modifications are expected to have a strong impact on the electronic/magnetic properties as well as charge transport capability of the resulting Por-GNR hybrids.

Acknowledgements

Conflict of interest

The authors declare no conflict of interest.

[1]   a) R. Lindner, A. Kühnle, *ChemPhysChem* **2015**, *16*, 1582-1592; b) S. Clair, D. G. de Oteyza, *Chem. Rev.* **2019**, *119*, 4717-4776; c) G. Franc, A. Gourdon, *Phys. Chem. Chem. Phys.* **2011**, *13*, 14283-14292.

RESEARCH ARTICLE

[2]   a) P. A. Held, H. Fuchs, A. Studer, *Chem. Eur. J.* **2017**, *23*, 5874-5892; b) J. Björk, F. Hanke, *Chem. Eur. J.* **2014**, *20*, 928-934.

[3]   a) D. G. de Oteyza, P. Gorman, Y.-C. Chen, S. Wickenburg, A. Riss, D. J. Mowbray, G. Etkin, Z. Pedramrazi, H.-Z. Tsai, A. Rubio, M. F. Crommie, F. R. Fischer, *Science* **2013**, *340*, 1434-1437; b) L. Gross, F. Mohn, N. Moll, P. Liljeroth, G. Meyer, *Science* **2009**, *325*, 1110-1114.

[4]   L. Grill, M. Dyer, L. Lafferentz, M. Persson, M. V. Peters, S. Hecht, *Nat. Nanotechnol.* **2007**, *2*, 687.

[5]   a) M. Lackinger, *Chem. Commun.* **2017**, *53*, 7872-7885; b) Q. Sun, L. Cai, H. Ma, C. Yuan, W. Xu, *ACS Nano* **2016**, *10*, 7023-7030; c) N. Kocić, X. Liu, S. Chen, S. Decurtins, O. Krejčí, P. Jelínek, J. Repp, S.-X. Liu, *J. Am. Chem. Soc.* **2016**, *138*, 5585-5593.

[6]   a) A. Hirsch, *Nat. Mater.* **2010**, *9*, 868; b) Q. Sun, R. Zhang, J. Qiu, R. Liu, W. Xu, *Adv. Mater.* **2018**, *30*, 1705630.

[7]   J. Cai, P. Ruffieux, R. Jaafar, M. Bieri, T. Braun, S. Blankenburg, M. Muoth, A. P. Seitsonen, M. Saleh, X. Feng, K. Müllen, R. Fasel, *Nature* **2010**, *466*, 470.

[8]   M. Treier, C. A. Pignedoli, T. Laino, R. Rieger, K. Müllen, D. Passerone, R. Fasel, *Nat. Chem.* **2010**, *3*, 61.

[9]   Y. C. Chen, D. G. de Oteyza, Z. Pedramrazi, C. Chen, F. R. Fischer, M. F. Crommie, *ACS Nano* **2013**, *7*, 6123-6128.

[10] a) J. Cai, C. A. Pignedoli, L. Talirz, P. Ruffieux, H. Söde, L. Liang, V. Meunier, R. Berger, R. Li, X. Feng, K. Müllen, R. Fasel, *Nat. Nanotechnol.* **2014**, *9*, 896; b) H. Zhang, H. Lin, K. Sun, L. Chen, Y. Zagranyarski, N. Aghdassi, S. Duhm, Q. Li, D. Zhong, Y. Li, K. Müllen, H. Fuchs, L. Chi, *J. Am. Chem. Soc.* **2015**, *137*, 4022-4025.

[11] P. Ruffieux, S. Wang, B. Yang, C. Sanchez-Sanchez, J. Liu, T. Dienel, L. Talirz, P. Shinde, C. A. Pignedoli, D. Passerone, T. Dumslaff, X. Feng, K. Mullen, R. Fasel, *Nature* **2016**, *531*, 489-492.

[12] a) O. Gröning, S. Wang, X. Yao, C. A. Pignedoli, G. Borin Barin, C. Daniels, A. Cupo, V. Meunier, X. Feng, A. Narita, K. Müllen, P. Ruffieux, R. Fasel, *Nature* **2018**, *560*, 209-213; b) D. J. Rizzo, G. Veber, T. Cao, C. Bronner, T. Chen, F. Zhao, H. Rodriguez, S. G. Louie, M. F. Crommie, F. R. Fischer, *Nature* **2018**, *560*, 204-208.

[13] L. Talirz, P. Ruffieux, R. Fasel, *Adv. Mater.* **2016**, *28*, 6222-6231.

[14] C. Bronner, S. Stremlau, M. Gille, F. Brauße, A. Haase, S. Hecht, P. Tegeder, *Angew. Chem. Int. Ed.* **2013**, *52*, 4422-4425.

[15] M. Di Giovannantonio, J. I. Urgel, U. Beser, A. V. Yakutovich, J. Wilhelm, C. A. Pignedoli, P. Ruffieux, A. Narita, K. Müllen, R. Fasel, *J. Am. Chem. Soc.* **2018**, *140*, 3532-3536.

[16] a) G. Sedghi, V. M. García-Suárez, L. J. Esdaile, H. L. Anderson, C. J. Lambert, S. Martín, D. Bethell, S. J. Higgins, M. Elliott, N. Bennett, J. E. Macdonald, R. J. Nichols, *Nat. Nanotechnol.* **2011**, *6*, 517; b) M. Jurow, A. E. Schuckman, J. D. Batteas, C. M. Drain, *Coord. Chem. Rev.* **2010**, *254*, 2297-2310.

[17] T. Tanaka, A. Osuka, *Chem. Soc. Rev.* **2015**, *44*, 943-969.

[18] a) G. Sedghi, L. J. Esdaile, H. L. Anderson, S. Martin, D. Bethell, S. J. Higgins, R. J. Nichols, *Adv. Mater.* **2012**, *24*, 653-657; b) V. S.-Y. Lin, M. J. Therien, *Chem. Eur. J.* **1995**, *1*, 645-651; c) H. L. Anderson, *Chem. Commun.* **1999**, 2323-2330.

[19] a) Y.-J. Chen, S.-S. Chen, S.-S. Lo, T.-H. Huang, C.-C. Wu, G.-H. Lee, S.-M. Peng, C.-Y. Yeh, *Chem. Commun.* **2006**, 1015-1017; b) V. Lin, S. DiMagno, M. Therien, *Science* **1994**, *264*, 1105-1111.

[20] H. S. Cho, D. H. Jeong, S. Cho, D. Kim, Y. Matsuzaki, K. Tanaka, A. Tsuda, A. Osuka, *J. Am. Chem. Soc.* **2002**, *124*, 14642-14654.

[21] E. Leary, B. Limburg, A. Alanazy, S. Sangtarash, I. Grace, K. Swada, L. J. Esdaile, M. Noori, M. T. González, G. Rubio-Bollinger, H. Sadeghi, A. Hodgson, N. Agraït, S. J. Higgins, C. J. Lambert, H. L. Anderson, R. J. Nichols, *J. Am. Chem. Soc.* **2018**, *140*, 12877-12883.

[22] A. Tsuda, A. Osuka, *Science* **2001**, *293*, 79-82.

[23] a) J. Li, N. Merino-Díez, E. Carbonell-Sanromà, M. Vilas-Varela, D. G. de Oteyza, D. Peña, M. Corso, J. I. Pascual, *Sci. Adv.* **2018**, *4*, eaaq0582; b) W. Perkins, F. R. Fischer, *Chem. Eur. J.* **2017**, *23*, 17687-17691; c) J. Li, N. Friedrich, N. Merino, D. G. de Oteyza, D. Peña, D. Jacob, J. I. Pascual, *Nano Lett.* **2019**, *19*, 3288-3294; d) X. Su, Z. Xue, G. Li, P. Yu, *Nano Lett.* **2018**,

18, 5744-5751; e) Y. He, M. Garnica, F. Bischoff, J. Ducke, M.-L. Bocquet, M. Batzill, W. Auwärter, J. V. Barth, *Nat. Chem.* **2016**, *9*, 33.

[24] J. Hutter, M. Iannuzzi, F. Schiffmann, J. VandeVondele, *Wiley Interdisciplinary Reviews: Computational Molecular Science* **2014**, *4*, 15-25.

[25] G. Pizzi, A. Cepellotti, R. Sabatini, N. Marzari, B. Kozinsky, *Computational Materials Science* **2016**, *111*, 218-230.

[26] H. Lee, M. Jo, G. Yang, H. Jung, S. Kang, J. Park, *Dyes Pigm.* **2017**, *146*, 27-36.

[27] J. S. Lindsey, I. C. Schreiman, H. C. Hsu, P. C. Kearney, A. M. Marguerettaz, *J. Org. Chem.* **1987**, *52*, 827-836.

[28] P. H. Jacobse, A. van den Hoogenband, M.-E. Moret, R. J. M. Klein Gebbink, I. Swart, *Angew. Chem. Int. Ed.* **2016**, *55*, 13052-13055.

[29] a) N. Merino-Díez, A. Garcia-Lekue, E. Carbonell-Sanromà, J. Li, M. Corso, L. Colazzo, F. Sedona, D. Sánchez-Portal, J. I. Pascual, D. G. de Oteyza, *ACS Nano* **2017**, *11*, 11661-11668; b) H. Huang, D. Wei, J. Sun, S. L. Wong, Y. P. Feng, A. H. C. Neto, A. T. S. Wee, *Sci. Rep.* **2012**, *2*, 983.

[30] B. Cirera, B. de la Torre, D. Moreno, M. Ondráček, R. Zbořil, R. Miranda, P. Jelínek, D. Écija, *Chem. Mater.* **2019**, *31*, 3248-3256.

[31] S. Braun, W. R. Salaneck, M. Fahlman, *Adv. Mater.* **2009**, *21*, 1450-1472.

[32] P. Ruffieux, J. Cai, N. C. Plumb, L. Patthey, D. Prezzi, A. Ferretti, E. Molinari, X. Feng, K. Müllen, C. A. Pignedoli, R. Fasel, *ACS Nano* **2012**, *6*, 6930-6935.

[33] N. K. S. Davis, M. Pawlicki, H. L. Anderson, *Org. Lett.* **2008**, *10*, 3945-3947.

[34] N. K. S. Davis, A. L. Thompson, H. L. Anderson, *Org. Lett.* **2010**, *12*, 2124-2127.

[35] N. K. S. Davis, A. L. Thompson, H. L. Anderson, *J. Am. Chem. Soc.* **2011**, *133*, 30-31.

[36] S. Wang, L. Talirz, C. A. Pignedoli, X. Feng, K. Müllen, R. Fasel, P. Ruffieux, *Nat. Commun.* **2016**, *7*, 11507.

[37] J. van der Lit, M. P. Boneschanscher, D. Vanmaekelbergh, M. Ijäs, A. Uppstu, M. Ervasti, A. Harju, P. Liljeroth, I. Swart, *Nat. Commun.* **2013**, *4*, 2023.